University of Reading
School of Mathematics, Meteorology & Physics

Application of the Phase/Amplitude Method to the Study of Trapped Waves in the Atmosphere and Oceans

This dissertation is a joint MSc in the Departments of Mathematics & Meteorology and is submitted in partial fulfillment of the requirements for the degree of Master of Science

Dan Lucas

August 19, 2007

Contents

Introduction

The study of many oceanographic and atmospheric waves can be reduced to understanding solutions of the time independent Schrödinger equation.

$$\frac{d^2y}{dx^2} + [V(x) - \lambda$$

Schrödinger equation. This transforms equation (1) into a nonlinear ODE to be solved for either phase or amplitude. It is not usual to replace the solution of a linear ODE with the solution of a nonlinear one, however solving for phase and amplitude in this way is a more physically realistic approach since wave motions in an inhomogeneous domain, i.e. where the potential varies with x, will have a phase and amplitude also dependent on x. We consider solutions over the interval $[x_0, +\infty)$, thus we require at least three boundary conditions to find a unique solution since formulating the solution in terms of phase and amplitude as above is non-unique (e.g. $\Phi(x) = 0 \Rightarrow y(x) = A(x)$). A fourth order Runge-Kutta scheme is employed in the solution of the ODEs with a WKB type approximation to obtain initial conditions, at x_0, on phase and amplitude, which allow for smooth (non-oscillatory) solutions. The boundary condition "at infinity" is dealt the equator whilst propagating zonally around it. The analytic solutions in terms of parabolic cylinder functions presented by Matsuno (1966) [10] are used to test the methods.

The Schrödinger equation in the context of trapped lee waves is discussed in chapter 3. Here a linearised Boussinesq equation set is used to derive the Schrödinger equation for vertical wind speed with height, the potential in this case is the ‘Scorer parameter’, a function of mean horizontal wind speed and static stability with height. The horizontal wave number takes on the role of eigenvalue and resonance modes are computed from profiles of Scorer parameter. Known analytical solutions in terms of Bessel functions are used for comparison here, where the Scorer parameter profile is exponential. An observed profile of Scorer parameter is interpolated using cubic splines and the numerical methods are used to compute resonance modes.

Also included in this manuscript is a short section summarising the findings

Chapter 1

Numerical Method

As mentioned in the introduction the method used in this study will be the phase/amplitude method and results in solving an ODE system using standard numerical integration (4th order Runge-Kutta) with a shooting method on λ to fix the end boundary condition.

1.1 Deriving the phase/amplitude ODEs

Phase/Amplitude Approach:

$$A = \frac{A_0}{\sqrt{m}} \tag{1.1}$$

where A_0 is an arbitrary constant, without loss of generality we can set $A_0 = 1$. This allows for the elimination of A or m in the real part of the Schrödinger equation. Eliminating m gives

$$A \;\; + [V - \lambda]A = \frac{1}{A^3} \tag{1.2}$$

Milnes equation. Eliminating A yields

$$m \;\; - \frac{3m^{\;2}}{2m} + 2[m^2 + \lambda - V]m = 0 \tag{1.3}$$

Notice that in making this change of variable we have moved from having a linear ODE (1) to a nonlinear ODE, and in the process increased the number of boundary conditions required to obtain a unique solution. These equations remain to be solved to generate the general solution to equation (1) noting that for real solutions

$$y(x) \;=\; Y_0 A \sin\left(\int_{x_0}^{x} A^{-2}(x)dx + \Phi_0\right) \tag{1.4}$$

$$y(x) \;=\; Y_0 \frac{1}{\sqrt{m}} \sin\left(\int_{x_0}^{x} m(x)dx + \Phi_0\right) \tag{1.5}$$

for some x_0 in the interval and a constant arbitrary a. The Wronskian, a result from classical ODE theory is an invariant of this problem hence (pages 189-191 [14])

$$y_1(x)y_2(x) - y_2(x)y_1(x) \equiv a \tag{1.6}$$

Defining $w(x)$ as

$$w(x) = \left[y_1^2(x) + y_2^2(x) \right]^{1/2}$$

, differentiating twice and eliminating $y_1(x)$ and $y_2(x)$ using equation (1) and simplifying by using equation (1.6) we obtain the so called "Milne's equation"

$$\frac{d^2w}{dx^2} + [V(x) - \lambda]\, w = \frac{a^2}{w^3}$$

Note that this is analogous to equation (1.2) if $a = 1$ so that the function w and the amplitude A coincide in this case (alternatively make the transformation $w(x) \rightarrow a^{1/2}w(x)$). The general solution of the time independent Schrödinger equation is then

$$y(x) = Y_0 w(x) \sin\left(a \int_{x_0}^{x} w^{-2}(x')dx' - \Phi_0 \right) \tag{1.7}$$

where Y_0, a and Φ_0 are arbitrary constants (this can be seen by substituting into Milne's equation to recover the Schrödinger equation). Note a cosine yields an equally valid solution corresponding to $\Phi_0 \rightarrow \Phi_0 - \pi/2$

1.2 Solving the phase/amplitude ODEs

$$y_{n+1} = y_n + \frac{dx}{6}(k_1 + 2k_2 + 2k_3 + k4)$$

where $y_n = y(ndx)$, n is the step, and the k's are given by

$$\begin{aligned}
k_1 &= f(ndx, y_n) \\
k_2 &= f\left(ndx + \frac{dx}{2}, y_n + \frac{dx}{2}k_1\right) \\
k_3 &= f\left(ndx + \frac{dx}{2}, y_n + \frac{dx}{2}k_2\right) \\
k_4 &= f(ndx + dx, y_n + dxk_3)
\end{aligned}$$

$$\Phi(x) = \int_{x_0}^{x} m(x\,;\lambda)dx = k\pi + \int_{x}^{+\infty} m(x\,;\lambda)dx$$

where $R = \int_{x}^{+\infty} m(x\,;\lambda)dx$ is the 'Residual'. Thus, assuming $\Phi_0 = 0$

$$\sin \left(\int_{x_0}^{x} m(x\,;\lambda)dx \right.$$

or a Newton-Raphson solver or a combination thereof [1]. Traditionally the shooting method for solving boundary value problems involves iterating on the derivative initial condition to converge on the end boundary condition.

In general for the phase/amplitude method we employ Newton-Raphson iteration to converge on the eigenvalue λ, since by isolating the eigenmode with the boundary condition we eliminate the need for a close first guess on λ. We update λ for successive iterations by means of

$$\lambda_{new} = \lambda_{old} - \frac{R_X}{dR_X/d\lambda}$$

where X is the end of the region we are solving over thus R_X is the residual at X.

$$R_X = \int_{x_0}^{X} m(x;\lambda)dx - k\pi$$

Hence in the routine we have an iteration loop, on each pass solving the phase/amplitude ODE using the RK4 procedure with a new eigenvalue until the boundary condition is satisfied (see figure 1.1). We thus have a stopping criterion on the iteration loop that $y(X) <$ where is some small parameter. Note that the iteration uses the residual of the phase in the convergence of λ though the stopping criterion is not that the residual should tend to zero but that the final solution should. This is important since as the residual goes to zero, the amplitude tends to infinity (equation (1.12)). It was found that too small an would hamper convergence since the eigenvalues will converge at machine precision (double) before the residual has met the convergence criterion and thus no further iterations are possible. Careful analysis found that an optimum value was $\approx 10^{-8}$.

The iteration loop was bounded such that if it proceeded through 20 iterations, the method was deemed not to have converged to prevent the routine becoming stuck in an infinite loop.

From Korsch and Laurent (1981) [9] and earlier Yuan et. al. (1974) [16] we can derive an expression for $dR_X/d\lambda$ provided $A(x_0) = 0$ (i.e. that

[1] See [4] Section 3.1-3.3 & 8.8 and [3] Section 2.3 & 11.2

$V(x_0) = 0$. If this condition is not satisfied we use a finite difference, see later). Starting from the following equations

$$\begin{aligned}
\frac{\partial}{\partial x}\left(y\frac{dy}{d\lambda}\right) &= y\frac{\partial y}{\partial \lambda} + y\,\frac{\partial y}{\partial \lambda} \\
\frac{\partial}{\partial x}\left(y\,\frac{dy}{d\lambda}\right) &= y\,\frac{\partial y}{\partial \lambda} + y\,\frac{\partial y}{\partial \lambda}
\end{aligned}$$

where primes denote derivatives with respect to x. Now using these expressions and equation (1)

$$\frac{\partial}{\partial x}\left(y\,\frac{dy}{d\lambda} - y\frac{dy}{d\lambda}\right) = y^2\frac{\partial\,(V(x)-\lambda)}{\partial \lambda} = -y^2 \tag{1.13}$$

Using the phase amplitude solution

$$y(x) = Y_0 A(x)\sin\left(\int_{x_0}^{x} A^{-2}(x\,)dx\, - \Phi_0\right)$$

and without loss of generality set $Y_0 = 1$, then

$$\begin{aligned}
y\,\frac{dy}{d\lambda} - y\frac{dy}{d\lambda} &= \left(A\,\frac{\partial A}{\partial \lambda} - A\frac{\partial A}{\partial \lambda}\right)\sin^2(\Phi(x)-\Phi_0) \\
&\quad + \cos^2(\Phi(x)-\Phi_0)\frac{\partial(\Phi(x)-\Phi_0)}{\partial \lambda} \\
&\quad + \sin^2(\Phi(x)-\Phi_0)\frac{\partial(\Phi(x)-\Phi_0)}{\partial \lambda} \\
&\quad - A^2\cos(\Phi(x)-\Phi_0)\sin(\Phi(x)-\Phi_0)\frac{\partial A^{-2}}{\partial \lambda} \\
&= \left(A\,\frac{\partial A}{\partial \lambda} - A\frac{\partial A}{\partial \lambda}\right)\sin^2(\Phi(x)-\Phi_0) + \frac{\partial(\Phi(x)-\Phi_0)}{\partial \lambda} \\
&\quad - A^2\frac{\sin 2(\Phi(x)-\Phi_0)}{2}\frac{\partial A^{-2}}{\partial \lambda}
\end{aligned}$$

Now integrating equation (1.13) from x_0 to X, setting $\Phi_0 = \Phi(X)$ since Φ_0 is arbitrary and noting that we have made the assumption that we use the initial conditions laid out in section 1.3.1 and that $V(x_0) = 0$ we have

$$\frac{\partial \Phi(X)}{\partial \lambda} = \int_{x_0}^{X} A^2(x\,)\sin^2[\Phi(x\,)-\Phi(X)]\,dx\, + A^2(x_0)\frac{\partial A^{-2}(x_0)}{\partial \lambda}\frac{\sin 2\Phi(x)}{2}$$

Now applying the initial conditions we obtain

$$\frac{dR_X}{d\lambda} = \frac{\partial\Phi(X)}{\partial\lambda} = \int_0^X A^2(x)\sin^2(\Phi(x) - \Phi(X))\,dx + \frac{\sin(2\Phi(X))}{4\lambda} \quad (1.14)$$

It was found to be sufficient for this integral to be calculated using a simple composite trapezoidal rule (pages 516-517 [4]) namely

$$\int_0^X f(x)dx = dx\left(\frac{f(0)}{2} + \sum_{i=1}^{N-1} f(idx) + \frac{f(N)}{2}\right)$$

where dx is the step size and here

$$f(x) = A^2(x)\sin^2(\Phi(x) - \Phi(X))$$

We can then use equation (1.14) to converge upon a value for λ for which the solution satisfies the boundary conditions.

An alternative to this form of Newton iteration, where it is not possible to make the above calculation, is to use a backward finite difference for the derivative of the residual, i.e.

$$\lambda_{i+1} = \lambda_i - \frac{R(\lambda_i)(\lambda_i - \lambda_{i-1})}{R(\lambda_i) - R(\lambda_{i-1})}. \quad (1.15)$$

where i denotes the current iteration step. This is known as the secant method and is useful where no expression for $dR_X/d\lambda$ can be found. Notice, however, that this form requires two starting values in the numerical technique and is a less accurate approximation of $dR_X/d\lambda$ and as such does not allow as rapid a convergence as the explicit expression for $dR_X/d\lambda$. The Secant Method's convergence is superlinear, as opposed to standard Newton method whose convergence is quadratic. The benefit is, however, that fewer function evaluations are required; Newton requires R_X and $dR_X/d\lambda$ where Secant only requires R_X (see [4] pages 102-104 for further details). The Secant method, as with Newton, in general is reliant on a good first guess at λ.

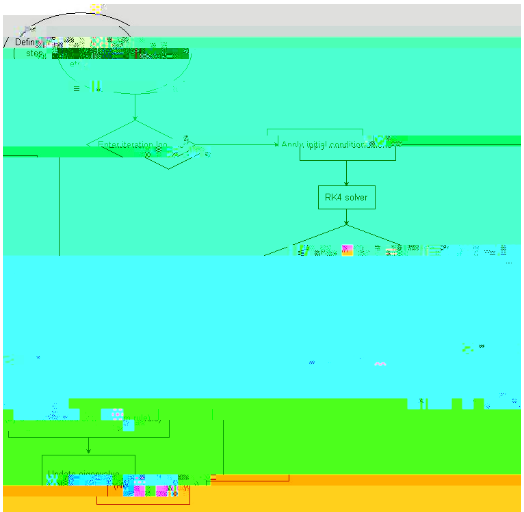

Figure 1.1: A Flow chart showing the steps in the phase amplitude routine.

1.5 MATLAB routine

Figure 1.1 is a flow chart outlining the stages involved in the phase/amplitude method routine. This was programmed in MATLAB and the code can be found in the appendix along with instructions on its use.

To allow objective assessment of the analysis which follow, it is important that we note machine precision. In MATLAB this is given by eps$= 2^{-52} = 2.22e-016$ and is defined as the distance from 1.0 to the next floating point number.

1.6 Alternative Numerical Methods

In order for this study to make good comparisons and conclusions about the accuracy and e□ciency of the phase/amplitude method it is necessary to consider other numerical techniques in use in the solution of the Schrödinger equation (1).

1.6.1 Standard disretisation

The standard way of solving a boundary value problem (BVP), where we have boundary data supplied at both ends of the region, is to express the ODE it terms of finite differences, e.g. the region $[0, X]$ is divided into $N = \frac{X}{h}$ intervals of length dx such that $x_i = idx$. This allows the approximation $y(x_i) \approx y_i$ to be made by finite differences. Taking central, second order, differences equation (1) can be replaced by

$$\frac{y_{i+1} - 2y_i + y_{i-1}}{dx^2} + (V_i - \lambda)y_i = 0$$

Now depending on the situation we are considering we will have boundary data to apply at either end of the interval, for example $y(x_0) = \alpha$, $y\ (x_0) = \beta$ etc. and similarly at $x =$ xx have $y(x_0) = 0$ we make $y_{-1} = y_1$. Thus in our A matrix we have an extra row for y_0 in which we impose this condition, resulting in the second entry being double since

$$\begin{aligned} \frac{y_{-1} - 2y_0 + y_1}{dx^2} + (V_0 - \lambda)y_0 &= 0 \\ \Rightarrow \frac{-2y_0 + 2y_1}{dx^2} + (V_0 - \lambda)y_0 &= 0 \end{aligned}$$

We can then employ the routines in MATLAB (`eig`) to compute the eigenvalues and solutions, note that such methods calculate N eigenvalues and eigenvectors which for high resolutions is quite computationally expensive. The task is, however made easier since the matrix A is tridiagonal, and in the Dirichlet case symmetric, meaning that no reduction to that form is required within the algorithm. Such a discretisation will result in a second order accurate solution due to the second order differencing.

1.6.2 Direct Shooting Method

As previously mentioned it is possible to discretise our region and directly solve equation (1) using a fourth order Runge-Kutta scheme with a shooting method on λ to fix the far boundary condition as in the phase/amplitude method by means of an iteration loop and a tolerance on $y(X)$. Without a means of specifying the mode, as we do with the boundary condition in the phase/amplitude method, the task of converging on the resonant modes becomes slightly more involved. A straight forward Newton solver has the drawback of requiring a close guess to converge upon or find a specific eigenvalue over neighbouring modes. However the typical way to circumvent this problem is to begin the routine with a few iterations of a bisection method (section 3.1 [4]). This entails beginning with an interval for λ i.e. $[\lambda_0, \lambda_1]$ and solving equation (1) to find the residual (in this case simply $y(X)$) for each end point, and the mid point $(\lambda_1 + \lambda_0)/2$. Then by examining the signs of the residues we can half the interval to contain the solution. In this way we can begin from a broad guess (or range) for λ and quickly find a closer estimate from which to begin the Newton iteration. If we use our fourth order RK-4 solver, this presents a more accurate method than the standard matrix eigenvalue technique described above. In comparison with the phase/amplitude method, a standard shooting method requires a secant method (with $y(X)$ taking the role of residual) in contrast to the straight forward Newton iteration for the phase/amplitude method which has an explicit expression for $dR/d\lambda$ (equation (1.14) when $V(x_0) = 0$).

As with the standard discretisation the form of the initial conditions is decided upon by the requirement of $y(x_0)$ to be zero or not. If not we impose a Neumann condition since $y(x_0)$ is unspecified by the problem. For the example of a symmetric potential, and hence solutions we would have

$$y(x_0) = 0 \quad , \quad y\ (x_0) \neq 0$$
$$y(x_0) \neq 0 \quad , \quad y\ (x_0) = 0$$

This method is more common place in the meteorological literature for solving eigenvalue problems of this type.

1.6.3 WKB approximation

The WKB approximation was introduced to allow us to set up our initial conditions, it can, however, yield an approximation for our solution in the region before any turning point of the potential.For example

$$y(x) = (V(x) - \lambda)^{-1/4} \sin\left(\int_{x_0}^{x} \sqrt{(V(x) - \lambda)}dx \right)$$

phase/amplitude method against known analytic solutions and the alternative methods outlined above, in accuracy, speed of convergence and resolution effects to validate its use in the study of such waves. It is also the intention of the author to provide some commentary of the findings, results and the wave motions themselves to provide a more thorough analysis of this methods worth.

Chapter 2

Equatorial Waves

The use of the Schrödinger equation in the study of trapped equatorial inertio-gravity [1], Kelvin and Rossby waves was first introduced by Matsuno (1966) [10] and later included in several texts concerned with the dynamics of the atmosphere and oceans (Gill [7], Holton [8]). The important feature at the equator is the vanishing of the Coriolis force, thus restricting geostrophic motions to higher latitudes. Matsuno's work involved a linearised shallow water equation model on a Cartesian coordinate system with a constant β-plane approximation (The Coriolis parameter is assumed proportional to latitude $f = \beta y$).

2.1 β-plane Derivation

Our equation set in this regime is

$$\begin{aligned} \frac{\partial u}{\partial t} - \beta y v + \frac{\partial \varphi}{\partial x} &= 0 \\ \frac{\partial v}{\partial t} + \beta y u + \frac{\partial \varphi}{\partial y} &= 0 \\ \frac{\partial \varphi}{\partial t} + gH\left(\frac{\partial u}{\partial x} + \frac{\partial v}{\partial y}\right) &= 0 \end{aligned}$$

[1] An inertio-gravity wave is simply a gravity wave of time and length scales sufficiently large as to allow the earth's rotation to effect their motions.

where (u, v) is the velocity vector, x denotes the longitudinal direction, y the meridional ($y = 0$ denoting the equator), $\varphi = gH$ is geopotential height, H the depth of the fluid layer, g the gravitational constant and $\beta = \frac{2\Omega}{a} = 2.3 \times 10^{-11} m^{-1} s^{-1}$ the β parameter at the equator, where a is the earth's radius and Ω the rotation rate..

Now we consider solutions of the form $e^{i(kx-\omega t)}$, that is wave solutions propagating zonally around the equator where k is a zonal wave number and ω angular frequency. i.e.

$$(u, v, \varphi) = (\hat{u}(y), \hat{v}(y), \hat{\varphi}(y))e^{i(kx-\omega t)}$$

with $\hat{u}, \hat{v}, \hat{\varphi}$ being y-dependent amplitudes. With these expressions our equation set becomes

$$-i\omega\hat{u} - \beta y\hat{v} + ik\hat{\varphi} = 0 \tag{2.1}$$

$$-i\omega\hat{v} + \beta y\hat{u} + \frac{d\hat{\varphi}}{dy} = 0 \tag{2.2}$$

$$-i\omega\hat{\varphi} + gH\left(ik\hat{u} + \frac{d\hat{v}}{dy}\right) = 0 \tag{2.3}$$

We now seek to eliminate $\hat{u}$ and $\hat{\varphi}$ to obtain an expression for $\hat{v}$. Substituting $\hat{u}$ from equation (2.1) into equation (2.3)

$$-i\omega\hat{\varphi} + gH\left(\frac{ik^2}{\omega}\hat{\varphi} - \frac{\beta k}{\omega}y\hat{v} + \frac{d\hat{v}}{dy}\right) = 0$$

Now differentiate and substitute for $\frac{d\hat{\varphi}}{dy}$ from equation (2.2)

$$\left(i\omega - gH\frac{ik^2}{\omega}\right)\beta y\hat{u} - gH\beta\frac{k}{\omega}y\frac{d\hat{v}}{dy} + \left(\omega^2 - gHk^2 - gH\beta\frac{k}{\omega}\right)\hat{v} + gH\frac{d^2\hat{v}}{dy^2} = 0 \tag{2.4}$$

Now substituting $\hat{\varphi}$ from equation (2.1) into equation (2.3) gives

$$-i\frac{\omega^2}{k}\hat{u} - \frac{\omega}{k}\beta y\hat{v} + gH\left(ik\hat{u} + \frac{d\hat{v}}{dy}\right) = 0 \tag{2.5}$$

which we can use to eliminate $\hat{u}$ in equation (2.4) to give us

$$\frac{d^2\hat{v}}{dy^2} + \left(\frac{\omega^2}{gH} - k^2 - \beta\frac{k}{\omega} - \frac{\beta^2 y^2}{gH}\right)\hat{v} = 0 \tag{2.6}$$

the time independent Schrödinger equation.

2.2 Analytic Solutions

Equation (2.6) can be recast into non-dimensional form via the following transformation to enable us to apply known analytic solutions for equations of this form (Holton [8]).

$$\tilde{y} = \left(\frac{\beta}{\sqrt{gH}}\right)^{1/2} y$$

Thus equation (2.6) becomes

$$\frac{d^2\hat{v}}{d\tilde{y}^2} + \left(\frac{\sqrt{gH}}{\beta}\left(\frac{\omega^2}{gH} - k^2 - \beta\frac{k}{\omega}\right) - \tilde{y}^2\right)\hat{v} = 0$$

For a classical Schrödinger equation with parabolic potential of the form

$$\frac{d^2Y}{dX^2} + \left(\lambda - X^2\right) Y - 0$$

solutions are well known in the form of parabolic cylinder functions (Abramowitz and Stegun [1] and Bateman [2]).

The classical result for eigenmodes decaying at infinity ($Y \to 0$ as $X \to \infty$) is that the eigenvalues take on the odd integers:

$$\lambda = 2n + 1 \qquad (n = 0, 1, 2...)$$

The parabolic cylinder functions in this case are given by

$$\hat{Y}(X) = Y_0 H_n(X) e^{-X^2/2} \qquad n = 0, 1, 2... \tag{2.7}$$

where $H_n(X)$ denotes the nth Hermite Polynomial, the first few being

$$H_0 = 1, \qquad H_1(X) = 2X, \qquad H_2(X) = 4X^2 - 2$$

and obeying the reccurence relation

$$H_{n+1} = 2XH_n(X) - 2nH_{n-1}(X)$$

Thus in the case of the trapped equatorial waves, the following relation follows [10]

$$\frac{\sqrt{gH}}{\beta}\left(\frac{\omega^2}{gH} - k^2 - \beta\frac{k}{\omega}\right) = 2n + 1 \qquad (n = 0, 1, 2, ...) \tag{2.8}$$

thus equation (2.6) becomes

$$\frac{d^2\hat{v}}{d\tilde{y}^2} + \left(2n + 1 - \tilde{y}^2\right)\hat{v} = 0 \tag{2.9}$$

And the parabolic cylinder functions are similarly

$$\hat{v}(\tilde{y}) = v_0 H_n(\tilde{y})e^{-\tilde{y}^2/2} \qquad n = 0, 1, 2... \tag{2.10}$$

Figure 2.1 shows the first three solutions. Notice that even n recover even solutions and odd n the odd solutions.

2.3 Numerical Solutions

These analytic solutions provide a useful means of testing and validating our phase/amplitude method and comparing it against the alternative numerical techniques. The numerical results presented will be solutions of the non-dimensional equation (2.9) and as such we will have in general the dispersion relation

$$\lambda = \frac{\sqrt{gH}}{\beta}\left(\frac{\omega^2}{gH} - k^2 - \beta\frac{k}{\omega}\right) = 2n + 1 \tag{2.11}$$

as eigenvalue and potential $V(x) = -\tilde{y}^2$.

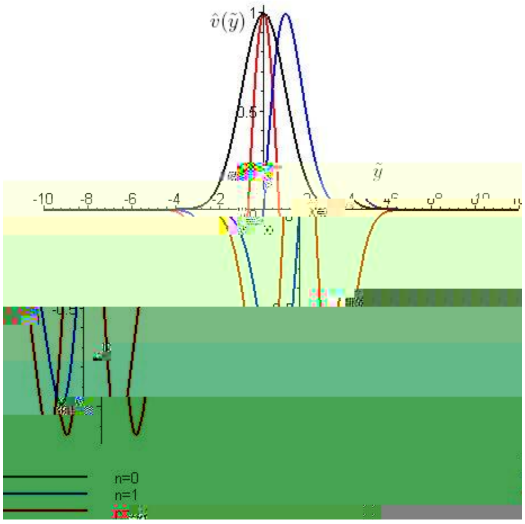

Figure 2.1: Exact Solution of equation (2.2) in terms of Hermite Polynomial solutions in Non-dimensional coordinates.

Mode n	Phase/Amplitude	Std Shooting	Matrix Eigenvalue
0	1.8e-009	2.7e-010	-0.011
1	4.0e-009	1.6e-009	3.1e-005
2	3.3e-009	6.8e-009	-0.028
3	6.6e-009	1.8e-008	1.6e-004
4	4.1e-009	3.8e-008	-0.038

Table 2.1: Accuracy of computed eigenvalues for the various methods $|2n + 1 - \lambda|$. Integration length $X = 7$, step size $dy = 0.01$.

Mode n	Phase/Amplitude	Std Shooting	Matrix Eigenvalue
0	1.6e-005	1.0e-006	0.12
1	3.3e-005	1.5e-005	3.1e-003
2	2.4e-005	6.6e-005	0.28
3	5.4e-005	1.8e-004	1.5e-002
4	2.8e-005	3.7e-004	0.36

Table 2.2: Accuracy of computed eigenvalues for the various methods $|2n + 1 - \lambda|$. Integration length $X = 7$, step size $dy = 0.1$.

2.3.1 Accuracy of λ & Resolution

Tables 2.1 and 2.2 show the accuracy of λ for the three methods under consideration namely the phase/amplitude method, the direct shooting method and the BVP matrix eigenvalue method for step size $dx = 0.01$ and $dx = 0.1$ respectively. The interval was chosen to be $[0, 7]$ such that we integrate in both directions about the equator. Notice however that the solutions are symmetric/antisymmetric about the equator, thus it is really only necessary to integrate in one direction. This interval also encompasses the interesting behaviour of the first 5 modes, as it is far enough past the turning points to ensure we include the decaying behaviour. The step sizes are chosen as a compromise between accuracy and computational expense. Recovering the odd modes (odd n) relies on setting $\Phi_0 = \pi/2$, as described in discussing a symmetric potential.

The results indicate that the phase/amplitude method is more consistently accurate on increasing n compared to the standard shooting method. The error is expected to increase with increasing n as the number of oscillations in the solution increase, this effect seems to be less evident with the phase/amplitude method. It is not clear on first impression that it is in evidence at all, however if we notice the distinction between odd and even solutions, they follow the trend independently of each other while remaining comparable in order of magnitude. Interestingly the standard shooting method is the method of choice for the lowest values of n, however as n increases the error also increases significantly.

The phase/amplitude method and standard shooting method both use a fourth order solver and this is borne out in comparing the error between the step sizes, four orders of magnitude are lost in error by a single order of magnitude reduction in step size.

The matrix method does not show easy comparisons. Firstly there is a considerable difference between the odd and even solutions. This can only be attributed to the treatment of the boundary condition, where Dirichlet data recovers the odd solutions and Nuemann the even. This is also the same treatment used in the standard shooting method, but clearly accuracy is compromised by approximating this boundary data via a second order finite difference as described in section 1.6. Thus we see the odd solutions being more accurate and conforming to the second order accuracy with the change in step size. The even solutions are far less accurate and are also not second order accurate.

2.3.2 Convergence

Mode n	Phase/Amplitude Iterations (Newton)	Phase/Amplitude Iterations (secant)	Std Shooting Iterations
0	9	10	11
1	6	7	11
2	5	7	11
3	5	7	11
4	5	7	11

Table 2.3: Number of iterations for convergence for the phase/amplitude for Newton and secant solvers and shooting method (including bisection iterations). X integration length as in table 2.1 with $dy = 0.01$.

Table 2.3 shows the number of iterations required for convergence of the two 'shooting' type methods. The phase/amplitude method is an improvement in this respect, converging with fewer iterations compared to the standard shooting method. The Newton iteration using equation (1.14) improves the method further over the secant method, equation (1.15) as expected. It was also noticed during the course of these tests that a change in the resolution had no effect on the number of iterations required for convergence and also that using the secant or Newton iteration in the phase amplitude method had no impact on its accuracy. As with accuracy it seems that the phase/amplitude method is not so efficient at the lower modes, especially $n = 0$. This may be in part due to integrating far past the turning point in this case, since the interval for the tests was $[0, 7]$ for all modes. Reducing this to $[0, 5]$ for $n = 0$ reduced the required iterations to 8, while the accuracy remained as in table 2.1. It is interesting that the standard shooting method shows no distinction between the modes in terms of iterations needed for convergence.

The stopping criterion in general are tighter for the phase/amplitude method, despite the fewer iterations it takes for accurate convergence. The choices for the stopping criterion, based upon the error in the full solution as $x \to X$ is explored in more depth in the following section.

The phase amplitude method, in the test carried out here had an initial guess of $\lambda_0 = 10$ for each eigenmode with the boundary condition (1.11) being the mechanism for selecting between them.

The method for converging on the full set of resonant modes for the standard shooting method is in part from the initial conditions (distinguishing

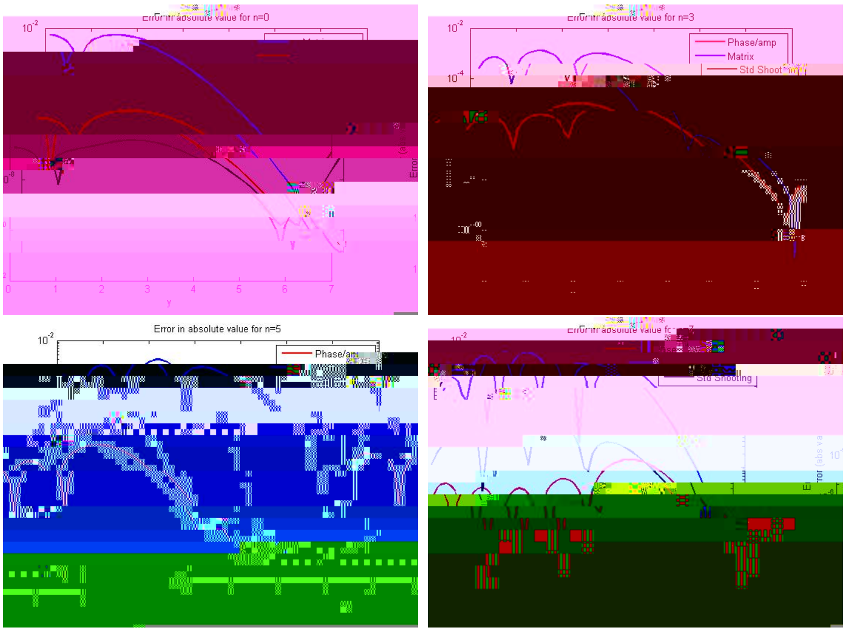

Figure 2.2: Error in absolute values of $\hat{v}$ of the numerical methods under consideration, compared to analytic solution (equation (2.10) for various n with non-dimensional $y = \tilde{y}$. $dy = 0.1$ (Logarithmic axis)

computations.

Table 2.4 shows the error in the computed solution for $\hat{v}(\tilde{y})$ under the L_2 norm. This is calculated by

$$||y_e - y_n||_{L2} = \sqrt{\int_0^X (y_e - y_n)^2 \, dx}$$

where y_e and y_n represent the analytic and numerical solutions respectively. This was computed using the composite trapezoidal rule as described in the first chapter. The error in the full solution was found to be quite sensitive to the stopping criterion. This is highlighted by the error for the $n = 0$ mode. From the plots in figure 2.2 and the error in the computed eigenvalue it appears that the standard shooting method is the more accurate method. However the L_2 norms suggest the phase/amplitude method to be more accurate. This is due to the phase/amplitude method being more accurate towards the end of the interval where $x \to X$ since it allows for a tighter

Mode n	Phase/Amplitude	Std Shooting	Matrix Eigenvalue
0	1.8e-019	1.7e-017	4.0e-008
1	1.8e-018	1.6e-018	1.7e-012
2			

2

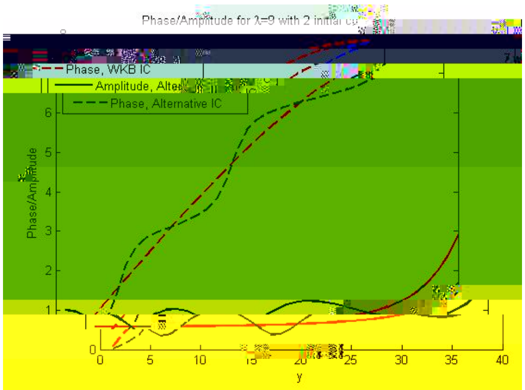

Figure 2.3: Phase and Amplitude for WKB initial conditions (equations 1.10), red, with initial conditions (2.12), blue. Non-dimensional $y = \tilde{y}$. $dy = 0.1$ $\lambda = 9$

conditions lead to a significant loss of accuracy and an increase in the number of iterations required for convergence.

2.4 Wave modes

Now we have obtained solutions to equation (2.6), both analytic and numerical, we can discuss the type of motions they present.

Equation (2.11) gives us a dispersion relationship between meridional mode, frequency and wavelength (longitudinal wave number). This is in the form of a cubic in ω and as such we will find three roots, for specified k and n ($n \geq 1$), corresponding to three forms of wave motion that are permitted at the equator under this model, those being a westward and an eastward propagating inertio-gravity wave at higher frequencies and a Rossby wave typically of a lower frequency. It is possible to highlight the distinction between the wave types by making the following approximations for wave frequencies, noting that for inertio-gravity wave the term ω/k will be small and for Rossby waves ω^2 will be small compared to the other terms. T90(t9o(t)1(he:t)28(vit)7

$$
\begin{aligned}
\omega_{1,2} &\approx \mp \sqrt{gH\left(k^2 + \frac{\beta}{\sqrt{gH}}(2n+1)\right)} \\
\omega_3 &\approx \frac{k}{\frac{k^2}{\beta} + \frac{2n+1}{\sqrt{gH}}}
\end{aligned}
\tag{2.13}
$$

where $\omega_{1,2}$ denote the inertio-gravity wave frequencies and ω_3 the Rossby wave frequency. Now observing the phase velocities of the full dimensioned parameters

$$
\begin{aligned}
c_{1g2} &\approx \mp c_g \sqrt{1 + \frac{k^2\beta}{c_g}(2n+1)} \\
c_3 &\approx \frac{-\beta}{k^2 + \frac{\beta}{c_g}(2n+1)}
\end{aligned}
$$

where $c_g = \sqrt{gH}$ is the phase speed of pure gravity waves.

Gill [7] gave bounds on the error for these approximations. For $n = 1$ the maximum fractional error on ω is 13% for inertio-gravity waves and 2% for Rossby waves. Our phase/amplitude method, having proven it's accuracy in calculating λ, can also be adapted to obtain specific frequencies of waves given a certain wave number by shooting on ω as opposed to λ. This allows us to calculate the specific frequencies for the different wave motions without the use of these approximations. This, however, presents the problem that the potential and phase are not seperable and thus the secant method described in section 1.4 needs to be employed.

Figure 2.4 is taken from Matsuno (1966) [10] and shows the allowed frequencies and wave number relationships for $n = 0, 1, 2$.

An interesting feature which Matsuno found was the behaviour of the waves of the $n = 0$ mode. The westward propagating inertio-gravity wave and the Rossby wave were found not be be entirely distinct, in that the frequencies of the two wave motions overlap. This has lead to this equatorial mode being referred to as a "Rossby-gravity" type wave. For $n = 0$ equation (2.11) becomes

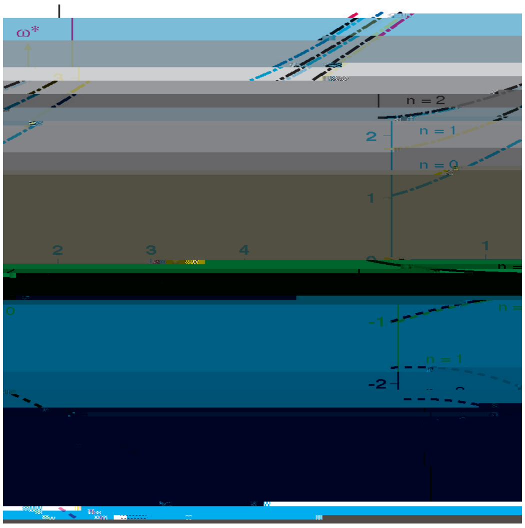

Figure 2.4: Dispersion diagram for equatorial waves with non-dimensional frequency and wave number ($k \;\; = k(\sqrt{gH}/\beta) \qquad \omega \;\; = \omega(\beta\sqrt{gH})$). Dashed

$$u = \frac{\sqrt{\beta/c}}{i\,(k^2 - \omega^2/c^2)}\left[\frac{\omega}{c}\tilde{y}\hat{v} - k\frac{d\hat{v}}{d\tilde{y}}\right]\exp i(kx - \omega t) \qquad (2.14)$$

$$\varphi = \frac{\sqrt{\beta/c}}{i\,(k^2 - \omega^2/c^2)}\left[\frac{ck}{\omega}\tilde{y}\hat{v} - \frac{d\hat{v}}{d\tilde{y}}\right]\exp i(kx - \omega t) \qquad (2.15)$$

$$v = \hat{v}\exp i(kx - \omega t) \qquad (2.16)$$

and observe from these the type of motions we expect from the waves we are considering.

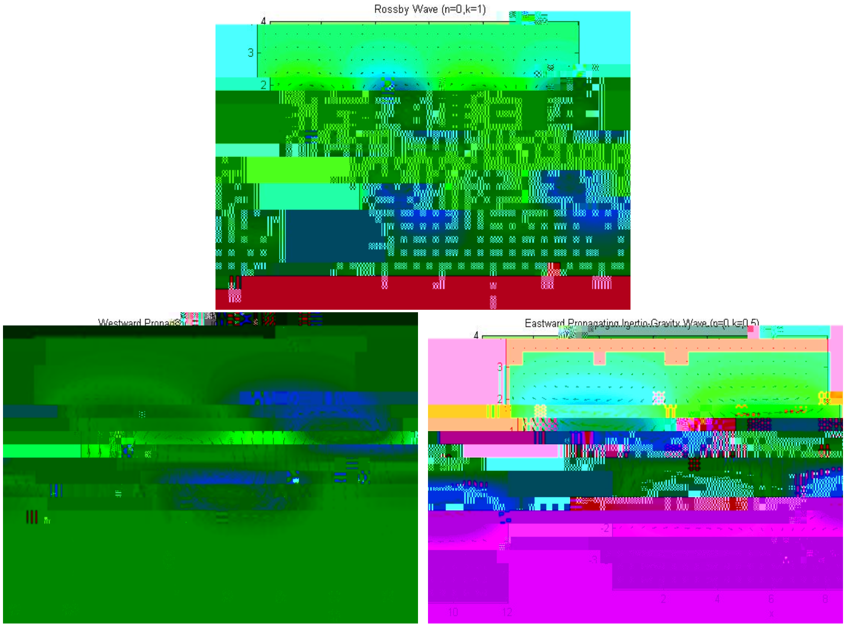

Figure 2.5: Pressure distribution (colour) and velocity vectors for $n = 0$ mode for $k = 0.5$ Rossby wave upper panel,$k = 1$ westward propagating inertio-gravity wave and eastward propagating inertio-gravity wave bottom panel. Non-dimensional coordinates.

Figure 2.6 shows the geopotential height and wind vector distributions for the three wave types for $n = 1$ and $n = 2$. It is expected that geostrophic motions will break 76.99860s.44099860eost301(three860equ]TJ-he)-301(wherree860three860Cor30 is that the Rossby waves of the $n = 1$ and $n = 2$ modes show a degree of geostrophy, shown up especially by the strong zonal winds about the equator. We also observe vortices about the equator in the $n = 2$ case brought about by the vanishing f. The gravity waves in these cases are certainly more ageostrophic by comparison.

The more interesting case is that of $n = 0$. From our previous analysis of frequencies we expect for larger k Rossby wave motions to replace the geexp We alsn

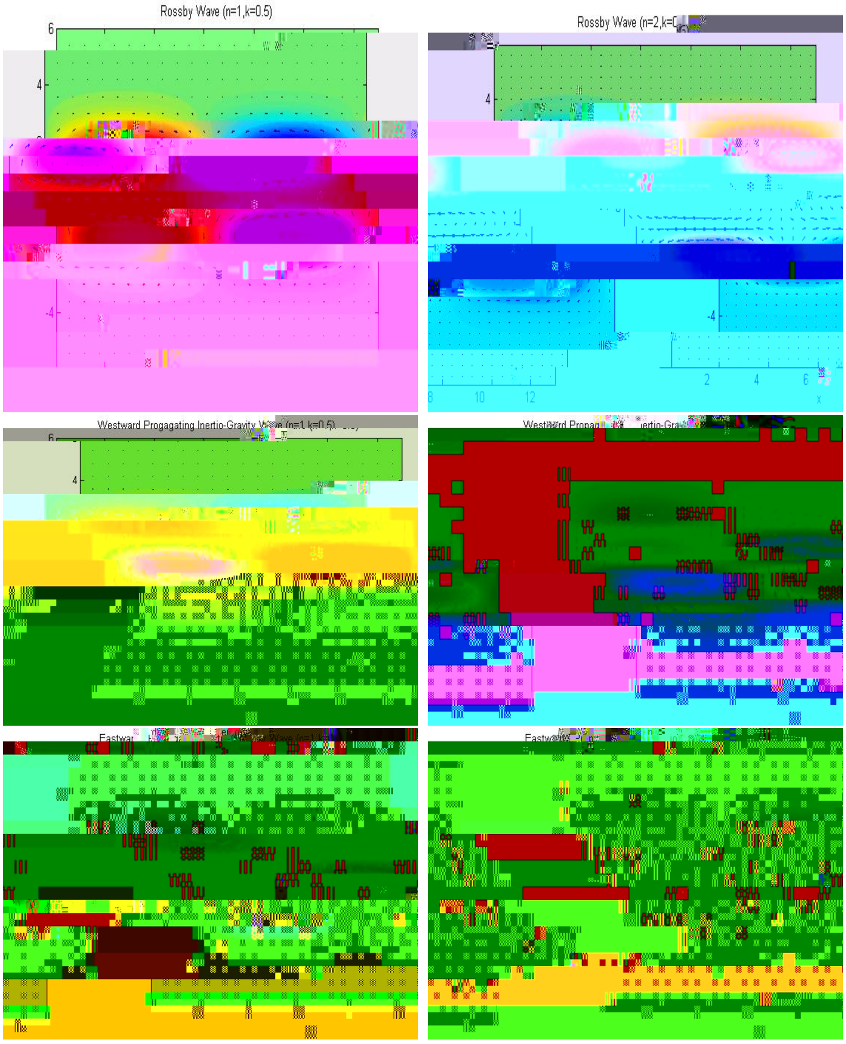

Figure 2.6: Pressure distribution (colour) and velocity vectors for $n = 1$ mode (left) and $n = 2$ (right) for $k = 0.5$. Rossby wave upper panel, westward propagating inertio-gravity wave middle panel and eastward propagating inertio-gravity wave bottom panel. Non-dimensional coordinates.

Chapter 3

Lee Waves

Despite of the relative smoothness of the globe, the atmosphere is so shallow that the mountains and ridges on its surface can penetrate into a significant proportion of it's depth. The atmosphere is for the most part stably stratified and thus sensitive to vertical motion, forced in this case by orography. The lee wave is a standing gravity wave where by a disturbance arising, usually from some isolated orography (e.g. a mountain), is propagated through the atmosphere via buoyancy. A stratified fluid at rest will tend to have any disturbances restored by the buoyancy force [15]. Such waves can have an impact on weather phenomena (clouds, turbulence etc.) and their development must be taken into consideration in numerical weather prediction, therefore it is important that accurate studies can be made. The Meteorological Office in the UK forecasts lee wave events for civil and military aviation, but severe gales resulting from a trapped lee wave event can also effect the surface, damaging property (e.g. Sheffield gale 16 Feb 1962)[13]. An untrapped lee wave disperses its energy vertically where it amplifies due to the decrease in density of the atmosphere with height. A trapped wave, however, is unable to disperse vertically due to a certain vertical structure of the atmosphere (see later) and amplifies via resonance with the orography underneath. [13]

3.1 The Linearised Boussinesq Equation Set

The derivation of the Schrödinger equation in the context of trapped lee waves follows from the linearised Boussinesq equation set ([8] pages 197-199). The Boussinesq approximation is that the density is assumed constant everywhere apart from in the buoyancy term in the vertical momentum equation. This means that the density is considered uniform and the model deals with small perturbations from this mean field, in effect removing the large static state of the atmosphere leaving only the interesting motions that we are concerned with.

We also neglect the effects of rotation, since the horizontal scales we are interested in will be small, and consider motion only in the x, z plane, with the x-axis aligned with the mean horizontal flow, to derive a diagnostic relationship between the vertical and horizontal wind perturbation fields. Therefore with $\mathbf{v} = (u, w)$ our starting equation set will be

$$\frac{D\mathbf{v}}{Dt} + \frac{1}{\rho}\nabla p + \mathbf{g} = 0 \tag{3.1}$$

$$\nabla.\mathbf{v} = 0 \tag{3.2}$$

$$\frac{D\theta}{Dt} = 0 \tag{3.3}$$

where $\frac{D}{Dt} = \frac{\partial}{\partial t} + \mathbf{v}.\nabla$.

Now for a stratified atmosphere we assume that the basic state of horizontal wind,temperature and pressure varies only with height and thus linearise our equation set by setting

$$\rho = \rho_0 + \rho$$

and we cancel the final two terms via equation (3.11).

then equation (3.14) will become

$$\frac{d^2W}{dz^2} + \left[l_s^2(z) - k^2 \right] W = 0 \tag{3.15}$$

and equation (3.15) becomes

$$c^2 \quad Z^2 \, d^2 W$$

converge upon allowed k

function solution. In this regime we find only two resonant modes in a physically reasonable domain. The second mode with a horizontal wavelength of $\lambda_1 = 13.2km$ is perhaps not as reasonable as the first, although in the interests of pragmatism, we shall assume that it is allowed to allow more analysis of the methods. The iterations to converge upon these modes is discussed in the following section.

3.3.1 Numerical Results

step size

It is the author's opinion that the phase/amplitude method, while being consistently numerically accurate, also allows for easier searching of the resonant modes. Both the direct shooting and Bessel function techniques require significantly more user input to specify the ranges of wave number to search

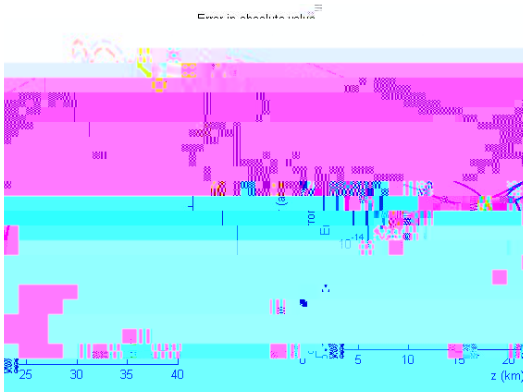

Figure 3.4: Absolute value of the error of the computed solution, $W(z)$ from the phase/amplitude method (red curves) and the direct shooting method (blue curves) when compared to bessel function solution. Dotted curves step size $dz = 0.1km$ and solid $dz = 0.01km$. $n = 2$, wavelength $= 13.2km$, integration length $X = 39km$,$l_S^2(0) = 1/5$, $c = 0.15$.(logarithmic axis)

in the higher mode, however the loss of accuracy at the end of the interval dominates for both methods.

3.4 Observed Scorer parameter profiles

Despite the analytic Scorer parameter profile providing a reasonable approximation and allowing a comparison with a known solution, it is preferable to obtain a more realistic form of $l_s(z)$ i.e. an observed profile. Shutts (1997) [13] describes making use of equation (3.15) in a code designed to forecast trapped lee wave events. This work uses second order finite differencing and a direct shooting method to calculate resonant modes, thus an improvement can be made by using the phase/amplitude method to perform this computation.

To employ the phase/amplitude method on a discrete profile, the observed data will need to be interpolated to define the profile at the desired resolution. This is achieved by means of cubic splines (MATLAB `spline` function) where a piecewise polynomial (cubic) representation interpolates between the data nodes. In some instances a smoothing process may also need to be carried out to obtain a sufficiently smooth and continuous representation of the Scorer parameter profile.

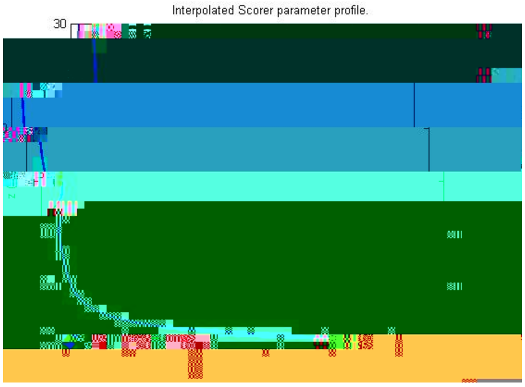

Figure 3.5: Cubic spline interpolated Scorer parameter profile ($l_S^2(z)$), resolution $dz = 1m$

Figure 3.5 shows the interpolated data. Observations of temperature, wind speed, pressure and height from a radiosonde sounding were used to calculate the Scorer parameter profile every $250m$

Conclusion

This work has involved a detailed study of the benefits of the phase/amplitude method over its contemporary numerical techniques in the solution of the time independent Schrödinger equation. This involved solving ODE's for phase and amplitude via a fourth order finite difference scheme (Runge-Kutta) and using a shooting method to fix the end boundary condition via Newton iteration. The boundary condition is formulated "at infinity" such that we have decaying behaviour in the region of negative potential, giving the solutions required in the study of atmospheric and oceanic trapped waves.

One set wave motions studied were trapped equatorial Rossby and inertio-gravity waves via a β-plane approximation, where analytic solutions exist [10]. The Schrödinger equation involves the meridional component of wind velocity and the potential here takes on a quadratic form, whereby the variation of coriolis force acts to trap wave motions about the equator. The eigenvalue of the problem is an expression involving the zonal frequency and wavenumbers. Exact solutions exist in the form of parabolic cylinder functions in this case and eigenvalues take odd integer values.

The other set of wave motions considered is that of trapped lee waves, or mountain waves, where stationary, internal gravity waves are forced by the orography. The derivation of the Schrödinger equation here involved the linearisation of the Boussineq equation set, under stationary conditions such that dependent variables are eliminated in favour of vertical wind speed. The resulting potential is commonly referred to as the Scorer parameter, a function of horizontal wind speed and static stability, with eigenvalue the horizontal wave number squared and under conditions where this decays with height trapped wave resonances occur. The work considers an analytic profile of Scorer parameter where known solutions exist in the form of Bessel functions, and accuracy and convergence comparisons are again made. Also a Scorer parameter profile involving observed data is interpolated and the numerical techniques are employed to solve and compute the resonance modes.

The results from the computations in the cases described above allow some analysis of the numerical techniques. It was found that the phase/amplitude method was more eﬀective for higher modes than is counterpart direct shooting method, although struggled somewhat with the lower modes. In the case of equatorial waves the lowest mode was an order of magnitude less accurate than the direct shooting method but in the lee wave case (analytic Scorer profile) the lowest modes were of comparable accuracy. The phase/amplitude method also showed an improvement in searching for resonant modes. The direct shooting approach requires a systematic method to search for the resonant modes, where the phase/amplitude method presents a more elegant method of isolating modes via the boundary condition.

It would be possible to extend the work on equatorial waves, using the

Acknowledgments

This work would not have been possible without the supervision of Rémi Tailleaux whose support, patience and advice has been invaluable. I would also like to thank Bob Lucas for his help with diagrams. The financial support provided by the Natural Environment Research Council for this MSc has been extremely important in the completion of this work.

Bibliography

[1] Abramowitz M., Stegun I.A., 1972: *Handbook of Mathematical Functions with Formulas, Graphs and Mathematical Tables.* National Bureau of Standards. Applied Mathematics Series- 55. 19.13

[2] Bateman, H., 1953: *Higher Transcendental Functions.* Volume II McGraw-Hill Book Company. 8.2

[3] Burden, R.L., Faires, J.D. 1997: *Numerical Analysis.* Sixth Edition. Brooks/Cole Publishing Company.

[4] Cheney, W., Kincaid, D., 1996: *Numerical Analysis. Mathematics of Scientific Computing.* Second Edition. Brooks/Cole Publishing Company.

[5] Erlick, C. et.al 2007: Linear waves in a symmetric equatorial channel. *Q. J. R. Meteorol. Soc. 133:571-577.*

[6] Foldvik, A. 1962: Two-dimensional mountain waves - a method for the rapid computation of lee wavelengths and vertical velocities. *Q. J. R. Meteorol. Soc. 88: 271-285.*

[7] Gill, A.E., 1982: *Atmosphere Ocean Dynamics.* International Geophysics Series. Volume 20. Academic Press. Sections 11.6,11.8

[8] Holton J.R., 2004: *An Introduction to Dynamic Meteorology.* Fourth Edition. International Geophysics Series. Volume 88. Elsevier Academic Press. Sections 7.4.2, 11.4

[9] Korsch, H. J., Laurent, H., 1981: Milne's di erential equation and numerical solutions of the Schrödinger equation I. Bound-state energies for single- and double-minimum potentials. *J. Phys. B: At. Mol. Phys. 14 (1981) 4214-4230.*

[10] Matsuno, T., 1966: Quasi-geostrophic motions in the equatorial area. *J. Met. Soc. Japan 44: 24-42.*

[11] Milne W.E., 1930: The Numerical Determination of Characteristic Numbers. *Physical Review. Volume 35. 863-867.*

[12] Smith, R. B. 1979: *The Influence of Mountains on the Atmosphere.* Advances in geophysics. Volume 21. 87-230

[13] Sutts, G. 1997: Operational lee wave forecasting. *Meteorol. App. 4, 23-25 (1997)*

[14] Trench W.F., 2000: *Elementary Di erential Equations.* Brooks/Cole Publishing Company.

[15] Wurtele M.G., Sharman R.D., Datta A., 1996: Atmospheric Lee Waves. *Annu. Rev. Fluid Mech. 1996.28/429-76.*

[16] Yuan J M, Lee S Y, Light J C, 1974: Reduced Fermion density matrices. II. Electron density of Kr. *J. Chem. Phys. 61 3394-400.*

Appendix A

MATLAB functions

A.1 Phase/Amplitude routine

```
%    msolve function for phase/amplitude method
%
%    To be used in conjunction with RKs 4th
%    order Runge-Kutta solver and associated functions.
%
%    Inputs are interval size, initial guess for eigenvalue
%    Phi_0, n mode, and resolution dx.
%
%    Outputs eigenvalue, solution, phase and amplitude
%
%%%%%%%%%%%%%%%%%%%%%%%%%%%%%%%%%%%%%%%%%%%%%%%%%%%%%%%%%%%%%%%


N=X0/dx;      %number of steps
e=0.000001;  %shooting method tolerance
a=1;          %iteration step
lambda(1)=L;
while (a<20) %iteration limit to prevent infinite loop

    A1(1)=(V(0,dx,lambda(a)))^(-0.25);  %initial conditions
    A2(1)=0; %equatorial case, derivative BC =0
    phi(1)=0;


    for
```

```
            break

        end



        r(a)=((phi(N)-phi_0)-n*pi); %compute residue

        %dR/d Lambda by composite trapezium rule
        D(1)=0;
        for K=2:(N-1)
            D(K)=(D(K-1)+(dx)*(d(A1(K),phi(K),phi(N))));
        end
        D1=D(N-1)+(dx/2)*(d(A1(N),phi(N),phi(N)))
                +sin(2*phi(N))/(4*V(0,dx,lambda(a)));

            %update lambda: Newton iteration.

            %secant method commented out
        %  if (n==1)
         % lambda(2)=lambda(1)+0.001;
        %else
         %   D=(r(n)-r(n-1))/(lambda(n)-lambda(n-1));
            lambda(a+1)=lambda(a)-r(a)/D1;
          % end


        a=a+1;
    end
    end




    function [a1,a2,phi]=RKs(A1,A2,Phi,i,dx,lambda)

    %%%%%%%%%%%%%%%%%%%%%%%%%%%%%%%%%%%%%%%%%%%%%%%%
    %
```

```
%      RK4 solver for system of equations in
%            phase/amplitude method
%
%      A1,A2,Phi from previous step,
%      i step index,
%      dx step length,
%      l eigenvalue.
%
%%%%%%%%%%%%%%%%%%%%%%%%%%%%%%%%%%%%%%%%%%%%%%%%

j1=dx*(f(A1));
k1=dx*A2;
l1=dx*g(A1,A2,i,dx,lambda);

j2=dx*(f(A1+k1/2));
k2=dx*(A2+l1/2);
l2=dx*g(A1+k1/2,A2+l1/2,i+1/2,dx,lambda);

j3=dx*(f(A1+k2/2));
k3=dx*(A2+l2/2);
l3=dx*g(A1+k2/2,A2+l2/2,i+1/2,dx,lambda);

j4=dx*(f(A1+k3));
k4=dx*(A2+l3);
l4=dx*g(A1+k3,A2+l3,i+1,dx,lambda);

j=(1/6)*(j1+2*j2+2*j3+j4);
k=(1/6)*(k1+2*k2+2*k3+k4);
l=(1/6)*(l1+2*l2+2*l3+l4);


a1=A1+k;
a2=A2+l;
phi=Phi+j;


end

```

```
function G=g(A1,A2,i,dx,lambda)
%function for RHS of second derivative

%solving for phase
%G=(3/2)*(A2^2/A1)-2*A1*(A1^2-V(i,dx,lambda,c));

 %solving for amplitude
G=1/(A1^3) -V(i,dx,lambda)*A1;

end



function v=V(i,dx,lambda)
%potential

v=-(i*dx)^2+lambda; %equatorial potential

end


function F=f(x)
%function for phase solution

%F=x;       %solving for phase
F=1/(x^2); %solving for amplitude
end


function D=d(A,phi,phiX)
%function to evaluate integrand in trapezium composite rule
% for dR/d lambda

D=(A^2)*((sin(phi-phiX))^2);
end
```

```
%%%%%%%%%%%%%%%%%%%%%%%%%%%%%%%%%%%%%%%%%%%%%%%%%

    Y1(1)=0;  %initial conditions
    Y2(1)=1;


```

```
            %RK4 call
            [YY1(K),YY2(K)]=
            RKS1(YY1(K-1),YY2(K-1),K-2,dx,lambda2);
    end
    %update interval
     if (sign(y1(X))==sign(YY1(X)))
        lambda1=lambda2;
        y1(X)=YY1(X);
     else
         lambda0=lambda2;
         Y1(X)=YY1(X);
     end
    end


lambda(2)=lambda1;
lambda(1)=lambda0;

%%%%%%%%%%%%%%%%%%%%%%%%%%%%%%%%%%%%%%%%%%%%%%%
%   Secant iterations
%%%%%%%%%%%%%%%%%%%%%%%%%%%%%%%%%%%%%%%%%%%%%%%%

while (n<20)

```

```
        lambda(n+1)=lambda(n)−Y1(n,X)/D;


    %break out of iteration loop once tolerance satisfied
    if (abs(Y1(n,X))<e)

         Y=Y1(n,:)/norm(Y1(n,:)); %normalise solution

        break
    end


    n=n+1;
end


function [y1,y2]=RKS1(Y1,Y2,n,dx,l)

%%%%%%%%%%%%%%%%%%%%%%%%%%%%%%%%%%%%%%%%%%%%%%%%%%
%
%     RK4 solver for system of equations
%           in shooting method
%
%     Y1,Y2 from previous step,
%     i step index,
%     dx step length,
%     l eigenvalue.
%
%%%%%%%%%%%%%%%%%%%%%%%%%%%%%%%%%%%%%%%%%%%%%%%%%%

k1=dx
```

```

k4=dx*(Y2+l3);
l4=dx*g1(Y1+k3,n+1,dx,l);

k=(1/6)*(k1+2*k2+2*k3+k4);
l=(1/6)*(l1+2*l2+2*l3+l4);


y1=Y1+k;
y2=Y2+l;


end

function G=g1(m1,i,dx,l)
%149
```

```
%initialise matrix A where AY=lambdaY
A(1,1)=-V(1,dx,0,0)-2/dx^2;
A(1,2)=1/dx^2;
A(2,1)=1/dx^2;
A(2,2)=-V(2,dx,0,0)-2/dx^2;

for
```

```
p=0;


%%%%%%%%%%%%%%%%%%%%%%%%%%%%%%%%%
%   Search for resonant modes

%   Bisection iterations
%%%%%%%%%%%%%%%%%%%%%%%%%%%%%%%%%
   z0=besselj(k0/c,ls/c);
   z1=besselj(k1/c,ls/c);

    if (sign(z0)==sign(z1))
        'poor interval'
        k=0;
        return
    end

    for k=1:3

        k2=k0+(k1-k0)/2;
       z2=besselj(k2/c,ls/c);

     if (sign(z1)==sign(z2))
        k1=k2;
        z1=z2;
     else
         k0=k2;
         z0=z2;
     end
    end


k(2)=k1;
k(1)=k0;

%%%%%%%%%%%%%%%%%%%%%%%%%%
%   Secant iterations
%%%%%%%%%%%%%%%%%%%%%%%%
```